

Magnetic Resonance Three-dimensional Cube Technique in the Measurement of Piglet Femoral Anteversion

Dong-Mei Sun¹, Shi-Nong Pan¹, En-Bo Wang², Li-Qiang Zheng³, Wen-Li Guo¹, Xi-Hu Fu¹

¹Department of Radiology, Shengjing Hospital of China Medical University, Shenyang, Liaoning 110004, China

²Department of Pediatric Orthopedics, Shengjing Hospital of China Medical University, Shenyang, Liaoning 110004, China

³Department of Clinical Epidemiology, Shengjing Hospital of China Medical University, Shenyang, Liaoning 110004, China

Abstract

Background: The accurate measurement of the femoral anteversion (FA) angle is always a topic of much debate in the orthopedic surgery and radiology research. We aimed to explore a new FA measurement method to acquire accurate results without radiation damage using piglet model.

Methods: A total of thirty piglets were assigned to two groups based on the age. Bilateral femora were imaged with 3.0-T magnetic resonance (MR) and 64-slice computed tomography (CT) examinations on all piglets. FA was measured on MR-three-dimensional (3D) postprocessing software with a four-step method: initial validation of the femoral condylar axis, validation of the condylar plane, validation of the femoral neck axis, and line-plane angle measurement of FA. After MR and CT examinations, all piglets were sacrificed and their degree of FA was measured using their excised, dried femora. MR, CT, and dried-femur measurement results were analyzed statistically; MR and CT measurements were compared for accuracy against each other and against the gold standard dried femur measurement.

Results: In both groups, the mean FA value measured by MR was lower than that measured by CT. A statistically significant difference was observed between CT- and dried-femur measurements but not between MR- and dried-femur measurements. A higher correlation (0.783 vs. 0.408) and a higher consistency (0.863 vs. 0.578) with dried-femur measurement results were seen for MR measurements than CT measurements in the 1-week age group. However, in the 8-week age group, similar correlations (0.707 vs. 0.669) and consistencies (0.864 vs. 0.821) were observed.

Conclusions: Noninvasive MR-3D-Cube reconstruction was able to accurately measure FA in piglets. Particularly in the 1-week age group with a larger proportion of cartilaginous structures, the correlation and consistency between MR- and dried-femur measurement results were higher than those between CT- and dried-femur measurements, suggesting that MR may be a new useful examination tool for FA-related diseases in children.

Key words: Femoral Anteversion; Hip; Magnetic Resonance Imaging; Piglet; Three-dimensional Fast Spin Echo Cube

INTRODUCTION

A normal femoral anteversion (FA) angle is an important factor in maintaining hip stability and normal gait in humans. Congenital or acquired hip diseases with abnormal FA often require surgical correction. Accurate determination of the FA is important in the effective treatment of these hip diseases and prevents serious complications from occurring.^[1-5] The accurate measurement of FA is always a topic of much debate in orthopedic surgery and radiology research.

The concept of FA may be traced back to 1954.^[6] Billing believed that FA was an included angle between the anteversion plane, formed by the axes of the femoral neck and the femoral shaft, and the condylar plane, formed by

the axes of the femoral condyle and the femoral shaft. This definition describes FA as an included angle between plane and plane. This concept has been used by many two-dimensional (2D) imaging methods for FA measurement such as radiography, fluoroscopy, ultrasound, and computed tomography (CT).^[7-13] The limitation of the above modalities

Address for correspondence: Dr. Shi-Nong Pan,

Department of Radiology, Shengjing Hospital of China Medical University,

No. 36, Sanhao Street, Heping, Shenyang, Liaoning 110004, China

E-Mail: cjr.panshinong@vip.163.com

This is an open access article distributed under the terms of the Creative Commons Attribution-NonCommercial-ShareAlike 3.0 License, which allows others to remix, tweak, and build upon the work non-commercially, as long as the author is credited and the new creations are licensed under the identical terms.

For reprints contact: reprints@medknow.com

© 2016 Chinese Medical Journal | Produced by Wolters Kluwer - Medknow

Received: 21-12-2015 **Edited by:** Li-Shao Guo

How to cite this article: Sun DM, Pan SN, Wang EB, Zheng LQ, Guo WL, Fu XH. Magnetic Resonance Three-dimensional Cube Technique in the Measurement of Piglet Femoral Anteversion. Chin Med J 2016;129:1584-91.

Access this article online

Quick Response Code:



Website:
www.cmj.org

DOI:
10.4103/0366-6999.184462

is that they use 2D measurements to evaluate a complex three-dimensional (3D) entity such as FA, which can directly affect the accuracy of the measurement results. We believe that a correct understanding of FA is the key to its accurate measurement. Due to the presence of individual variability in the neck-shaft angle, the true FA should be an angle formed by the femoral neck axis and the femoral shaft coronal plane, i.e., a line-plane angle. Only when the concept of FA as a line-plane angle is established can FA be measured more effectively and accurately.

In recent years, the 3D-CT technique has been widely used for FA measurement in hip studies.^[14-19] Compared with the previous examination methods, 3D-CT has the advantages of its ability to visualize the anatomic structure of the hip from any angle, its freedom from body position restrictions, and its high reproducibility. However, CT radiation exposure attracts more and more public concern, especially for children who are more sensitive to radiation damage than adults.^[20-25] Several 3D-CT examinations, including preoperative and postoperative evaluations, are often required in diseases such as developmental dysplasia of the hip, which has a relatively high incidence in infants.^[26] Just as Brenner concluded, each CT scan confers a very small increased risk of developing cancer in the future, but with hundreds of thousands of children getting CT scans every year that small individual risk balloons into a pressing public concern.^[27] Compared with CT, magnetic resonance (MR) examination has several advantages. First of all, MR can show cartilages on both ends of femur, which cannot be seen on CT. Meanwhile, radiation-free, multi-plane imaging, and high soft tissue resolution are also its advantageous places. Since 1990, several scholars^[12,28-30] have introduced MR techniques into the FA measurement field, but similar methods to 2D-CT and great dependence on patients' body position during the examination were limitations for them to acquire true FA.

Based on the concept of FA as a line-plane angle, our study was designed to explore a new FA measurement method to acquire accurate results without radiation damage. For this purpose, we introduced the MR-3D-fast spin echo (FSE)-Cube technique for volume scanning of piglet femur and then measured the FA in 3D space by the postprocessing software.

METHODS

Study design

Experiments were carried out on thirty healthy piglets with the approval of the Shengjing Hospital of China Medical University Institutional Animal Investigation Committee. The MR images were obtained with a GE 3.0-T MR scanner (Signa Excite HDx; GE Healthcare, Milwaukee, WI, USA) and the CT images were obtained with a 64-slice CT system (Philips Healthcare Company, Cleveland, USA). The piglets were then sacrificed and dissected and their femora were entirely removed for dried-femur measurement. After

the experiments were completed, FA was measured using MR and CT 3D postprocessing software.

Experimental animals

Experimental groups

Piglets were assigned to two groups on the basis of age, 15 in 1-week age group and 15 in 8-week age group. The inclusion criteria were normal development and gait by visual inspection, and normal shape and signal of pelvis and femur by MR coronal T1-weighted and T2-weighted imaging. The exclusion criteria were developmental malformations and claudicating gaits noted on visual inspection, and abnormal shape and signal of pelvis and femur on MR images.

Anesthetized procedures

All studies were performed under general anesthesia. The first anesthetic dose consisted of 40 mg of midazolam hydrochloride (Nhwa Pharmaceutical Co., Jiangsu, China) and 20 mg of ketamine hydrochloride (Gutian Pharmaceutical Co., Fujian, China) per kilogram of body weight, delivered by intramuscular injection. A second intramuscular anesthetic dose was given 30 min later, with 20 mg of ketamine hydrochloride and 5 mg of xylazine hydrochloride (Zizhu Pharmaceutical Co., Beijing) per kilogram of body weight. A continuous intravenous infusion of propofol (AstraZeneca PLC, London, UK) diluted in normal saline at a dose of 0.002 mg/kg per minute during the scanning sessions.

Magnetic resonance equipment and methods

All images were acquired with a 3.0-T MR imaging unit using an 8US TORSOPA coil (GE Healthcare, Milwaukee, WI, USA) with the experimental animals under anesthesia. The piglets were placed in the prone position, with their limbs fixed. The first step was the pelvis and femur routine examination, including coronal T1-weighted and T2-weighted imaging, for determining whether the piglets met inclusion criteria. The second step was 3D femoral volume scanning using the Cube technique, with a scanning range determined by the coronal localizer which covered the entire femur. Imaging with the 3D-FSE-Cube technique was performed using the following parameters: repetition time/echo time, 3000/106 ms; echo train length, 100; matrix, 224 × 224; field of view, 48 cm; section thickness, 1.4 mm; and receiver bandwidth, 62.5 kHz. All sections were acquired in 6 min.

The data were transmitted to a workstation (GE AW4.4, GE Healthcare) after scanning; then, postprocessing was conducted with 3D-maximum intensity projection software. The initial operation interface of the workstation was a quadrant interface, on which there were three display boxes [Figure 1], representing three series of orthogonal planes (box with yellow border; box with green border; and box with blue border). Each display box could show all planes parallel to the current plane by paging up and down. Two perpendicular lines within each box represented the corresponding of the other two boxes. For example, the green line in yellow box represented the intersection line of the current planes of green and yellow boxes; adjusting the direction of one line could

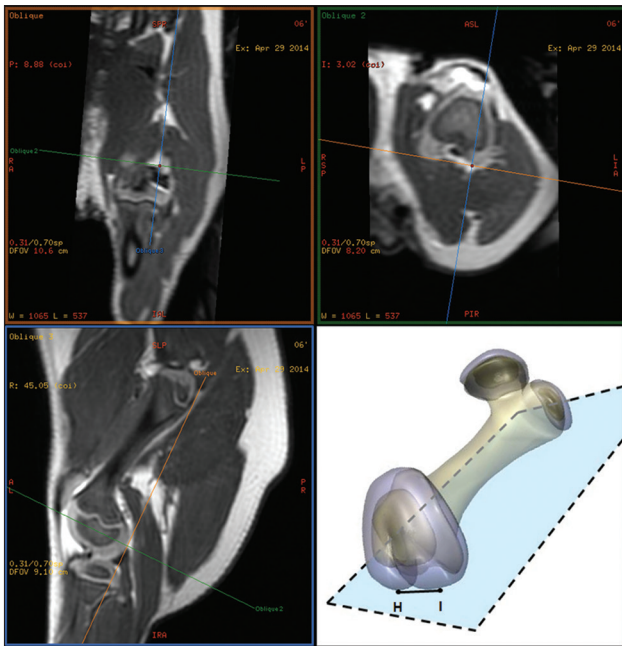


Figure 1: Initial validation of the condylar axis. The yellow line in the green box was the tangent line of the lowest points of the bilateral femoral condyles. Point H and I represented the two most posterior points of the femoral condyles in the stereogram, and the blue plane came close to the condylar plane.

change the direction of the plane it represented. The three series of planes were always orthogonal. Initially, we adjusted the position of the marked lines and enabled the three series of planes in each box to approximate the coronal, axial, and sagittal planes of the femur.

The FA measurement method was performed in four steps.

- Step 1: Initial validation of the condylar axis. An adjustment of the marked lines in yellow and green boxes was made so that the yellow line in green box became the tangent of the line connecting the 2 posterior femoral condyle margins; this line was determined by the lowest points of the bilateral femoral condyles. This provided the initial validation of the condylar axis [Figure 1].
- Step 2: Validation of the condylar plane. Keeping the intersection point on the condylar axis, the position of the upper part of the yellow line in blue box was adjusted [Figure 1] so that the yellow line passed through the lowest point of the greater trochanter. In Steps 1 and 2, it was little difficult to determine simultaneously the lowest points of the bilateral femoral condyles and the greater trochanter at once. However, after two or three times of adjustments, we found that the yellow lines passed through both the 2 lowest points of the femoral condyles and the greater trochanter in green and blue boxes simultaneously, and then the validation of the condylar plane was completed. The plane in yellow box was therefore the femoral coronal plane (condylar plane) [Figure 2].
- Step 3: Validation of the direction of the head-neck axis. The goal of this step was to find the plane passing through the femoral head-neck axis and was perpendicular to the condylar plane in yellow box. All adjustments in this

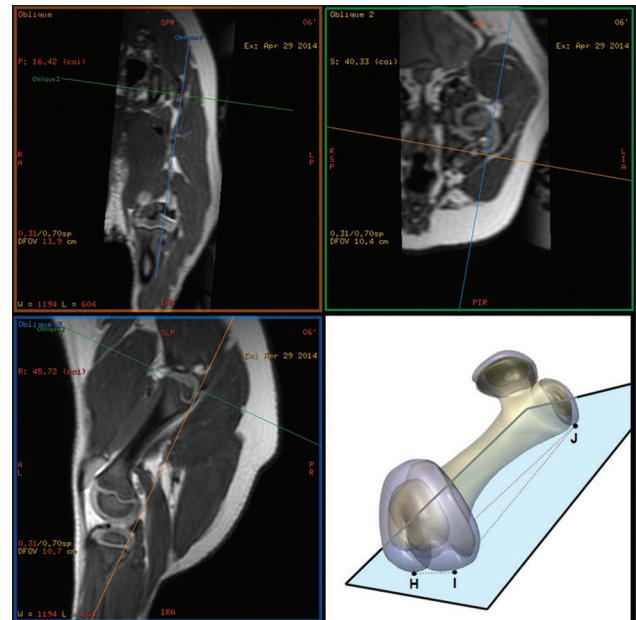


Figure 2: Validation of the condylar plane. The yellow lines were the tangent lines of the lowest points of the bilateral femoral condyles and the greater trochanter in the green and blue boxes. The two yellow lines determined the current plane in the yellow box, which was the femoral coronal plane (condylar plane). As it was shown in the stereogram, three points (point H and point I were the two most posterior points of the femoral condyles and point J was the most posterior point of the femoral greater trochanter) determined the blue plane (the condylar plane).

step were performed in yellow box. The central section of the femoral neck was first determined by paging up and down between the uppermost and lowermost femoral neck, then the intersection point of the 2 marked lines was fixed at the center point of the narrowest part of the femoral neck. With the same method, the center point of the widest part of the femoral head on the central section of the femoral head was found. The green line was then adjusted to pass through the above two points, so it represented the femoral head-neck axis. The current plane in green box was the plane which passed through the femoral head-neck axis and was perpendicular to the femoral coronal plane; its intersection line with the femoral coronal plane was the yellow line in green box [Figure 3].

- Step 4: FA measurement. The midpoints of the longest part of the femoral head and the shortest part of the femoral neck were determined in the current plane in box B [Figure 4]. The line connecting these 2 midpoints was the head-neck axis, and the included angle between this line and the yellow line was the FA.

All MR-3D postprocessing FA measurements were conducted independently by two experienced radiologists (Shi-Nong Pan and Dong-Mei Sun), and the mean value of three separate measurements was recorded.

Computed tomography equipment and methods

3D-CT scans were performed with a 64-slice CT machine. The scanning parameters were 120 kV and 150 mA, with

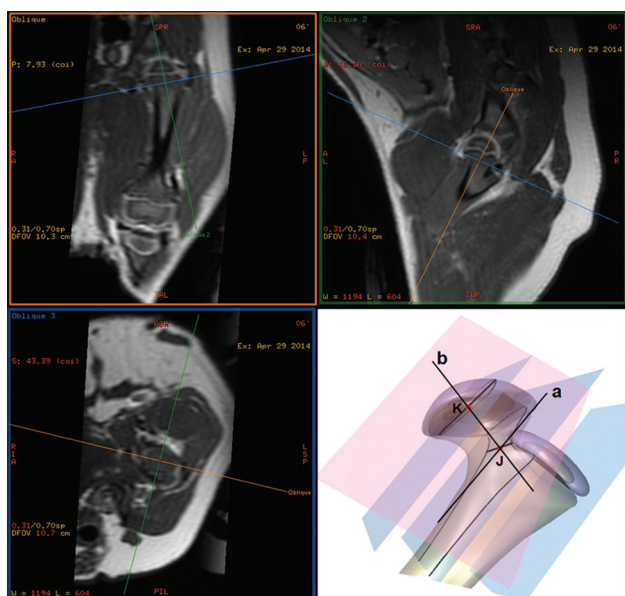


Figure 3: Validation of the direction of head-neck axis. The current plane in the blue box went through the head-neck axis and was perpendicular to the yellow box (the condylar plane) and their intersection line was the yellow line in the blue box. The stereogram showed how to find the current plane in the green box. All the blue planes presented the planes in the yellow box (that was paralleled to the condylar plane). The upper blue plane passed through the biggest section of the femoral head (with the central point K), and the mid blue plane passed through the smallest section of the femoral neck (with the central point J). Then, line b was the head-neck axis, and the pink plane (i.e., the current plane in the green box) went through line b and was perpendicular to the blue plane (the condylar plane). The two planes intersected at line a, which represented the yellow line in the current plane in the green box.

a 0.5 s rotation time. Contiguous slices at 1.0 mm intervals were obtained from the upper rim of the femoral head to the distal femur. The piglets were placed in the same position as in the MR examination. The images were retrospectively reconstructed at a CT workstation (Extended Brilliance workstation V3.5, Phillips Healthcare, Cleveland, USA) to produce the 3D images. The FA measurement methods adopted were those that had been widely used in current 3D-CT studies^[5,15,19] [Figure 5]. All CT postprocessing were conducted independently by the same radiologists (Shi-Nong Pan and Dong-Mei Sun), and the mean value of three separate measurements was recorded. Different processing orders were used to ensure that the radiologists did not know the corresponding MR results.

Dried-femur measurement method

After MR and CT examinations, the piglets were sacrificed with an intracardiac injection of 10 mg pentobarbital sodium (Xinya Pharmaceutical Co., Shanghai, China) per 5 kg of body weight. Their femora were entirely removed for evaluation.

First, the femur was placed on a horizontal table, with the bilateral posterior margins of the femoral condyles and the posterior margin of the greater trochanter contacting the table surface. Next, the femoral head was measured using

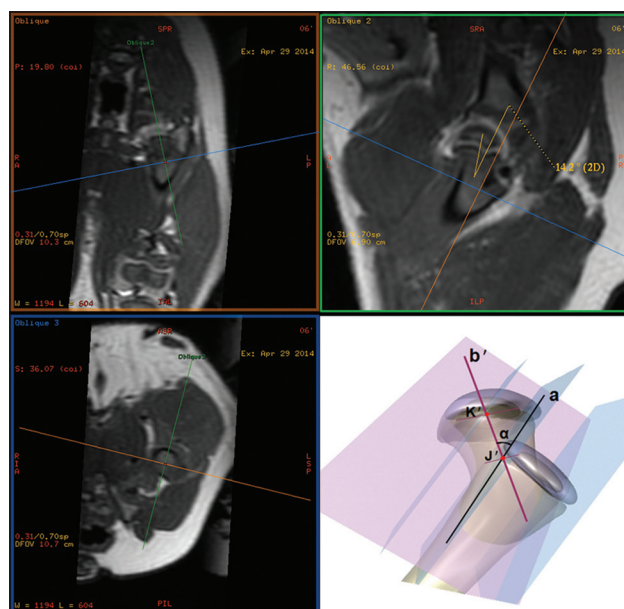


Figure 4: Validation of the head-neck axis and measurement of femoral anteversion. The midpoints of the longest part of the femoral head and the shortest part of the femoral neck were found out in the current plane in the green box. The included angle between the line connecting these two midpoints and the yellow line in the green box was femoral anteversion. As it was shown in the stereogram, the included angle between line b and line a both in the pink plane was the angle formed by the femoral head-neck axis and the femoral coronal plane, i.e., femoral anteversion.

a Vernier caliper, with the caliper's external measurement claw in line with the femoral head-neck axis. The midpoints of the longest part of the femoral head and the shortest part of the femoral neck were determined. The femoral head and neck were opened along the connecting line of these two midpoints, perpendicular to the table surface, with the greater trochanter preserved in order to determine the femoral coronal plane. The midpoints of the longest part of the femoral head and the shortest part of the femoral neck were determined again by measuring with a Vernier caliper, and the included angle between the connecting line of these 2 midpoints and the horizontal plane was designated as the FA. The FA was measured with a conimeter, with the bottom edge aligned to the connecting line of the above midpoints, and a deltoid plate, with one rectangular edge on the horizontal table and the other rectangular edge passing through the central point of the conimeter. Both the conimeter and the deltoid plate were perpendicular to the table surface. The angle indicated by the edge passing through the central point of the conimeter, -90° , was the value of FA [Figure 6]. The results of this measurement method were considered as the gold standard.

Statistical analysis

The formulation of statistical methods and the statistical analysis was both completed by a professional statistician (Li-Qiang Zheng) using Statistical Package for the Social Sciences software, version 17.0 (SPSS, Inc., Chicago, IL, USA). All continuous variables met Gaussian

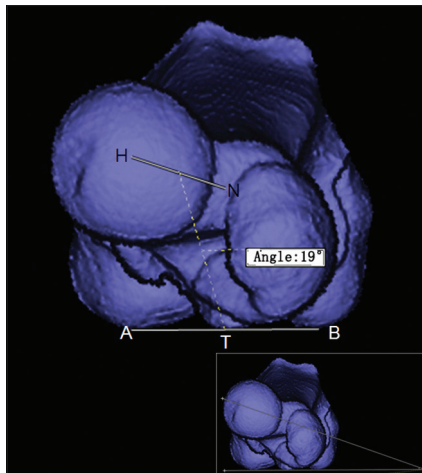


Figure 5: Computed tomography measurement method (only containing bony component).

distribution and homogeneity tests for variance and were therefore expressed as a mean \pm standard deviation (SD). Analysis of variance with randomized block design was performed for MR, CT, and dried-femur measurement results to determine whether the differences between the results of the three methods were statistically significant. Using the dried-femur measurement as the gold standard, Pearson's correlation coefficient analysis was conducted to determine the correlation between MR/CT measurement results and dried-femur measurement results. The intraclass correlation coefficient and Bland–Altman plots of the design data from the two-way mixed model were employed to analyze the consistency of MR and CT measurements with the gold standard. For all statistics reported, two-tailed tests with $P < 0.05$ were considered to indicate statistically significant differences.

RESULTS

The FA measurement results of the two piglet groups, by different methods, are shown in Table 1. In both age groups, the FA measurement results obtained by MR were lower than those by CT; the differences between MR and CT measurement results, and between CT and dried-femur measurement results, were statistically significant. No statistically significant difference was observed between MR and dried-femur measurement results.

The consistencies and correlations of CT and MR results with the gold standard measurements are demonstrated in Figures 7 and 8. In the 1-week age group, FA measurement results obtained by MR had better correlation with dried-femur measurement results than by CT (0.783 vs. 0.408) [Figure 7a and 7c]. Bland–Altman plots showed a measurement error of 9.4° between CT and the dried-femur measurement method, which was significantly greater than an error of -1.0° between MR and dried-femur measurement method [Figure 7b and 7d]. In the 8-week age group, FA measurement results obtained by MR were lower than those by CT, but MR and CT measurement

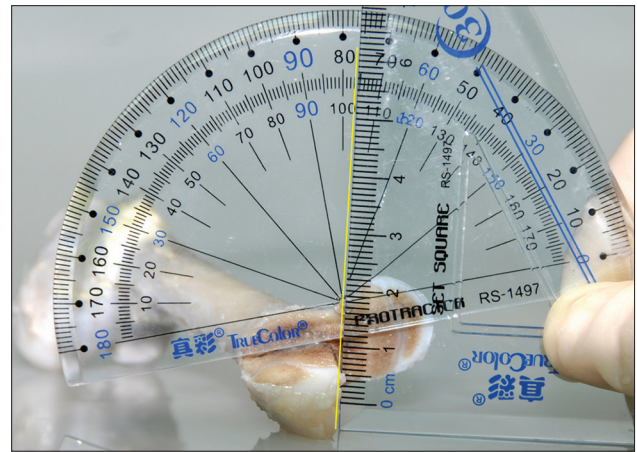


Figure 6: Physical measurement method. The femoral anteversion value = $104^\circ - 90^\circ = 14^\circ$. The femur was placed on the horizontal table, with the lowest points of the bilateral femoral condyles and the greater trochanter contacting the table surface. The bottom edge of a conimeter was aligned to the head-neck axis. The angle indicated by the rectangular edge of the deltoid plate passing through the central point of the conimeter (as was shown by the yellow line, 104°) $- 90^\circ$ was just femoral anteversion.

Table 1: FA values of different groups with different methods ($^\circ$)

Groups	<i>n</i>	MR	CT	Dried-femur measurement
1 week	15	17.23 \pm 2.32*	27.63 \pm 3.26 [†]	18.23 \pm 2.97
8 weeks	15	14.38 \pm 2.86 [‡]	20.80 \pm 3.21 [§]	15.13 \pm 2.13

Data were shown as mean \pm SD. * $P = 0.063$, compared with dried femora measurement; [†] $P < 0.001$, compared with dried femora measurement; [‡] $P = 0.110$, compared with dried femora measurement; [§] $P < 0.001$, compared with dried femora measurement. MR: Magnetic resonance; CT: Computed tomography; FA: Femoral anteversion; SD: Standard deviation.

results were both well-correlated with dried-femur measurement results (0.707 vs. 0.669) [Figure 8a and 8c]. Bland–Altman plots showed a greater measurement error for CT than for MR (5.7 vs. -0.8) [Figure 8b and 8d]. There was significantly higher consistency between MR and the dried-femur measurement results than between CT and the gold standard (0.863 vs. 0.578) in the 1-week age group; in the 8-week age group, there was similar consistency between MR/CT and dried-femur measurement results (0.864 vs. 0.821).

In 1-week and 8-week age groups, the mean CT radiation dose was 155 mGy/cm and 159 mGy/cm, respectively. The two-sample *t*-test showed no statistically significant difference in CT radiation dose between the groups ($t = 1.163$, $P = 0.255$).

DISCUSSION

Only sectional images are displayed using MR-3D postprocessing software for FA measurement and it is difficult to understand the 3D structure from these images. In order to facilitate the presentation, a schematic diagram was established that places the femur in a 3D coordinate

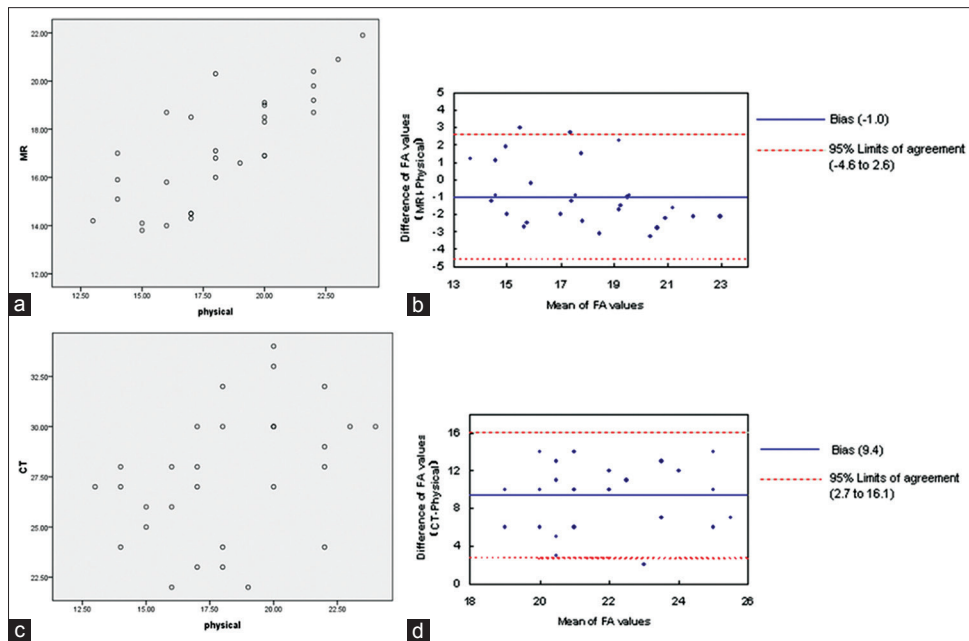


Figure 7: Correlation and Bland–Altman plots for 1-week group using magnetic resonance versus physical measurement (a and b) and computed tomography versus physical measurement (c and d). (a and c): the correlation between a trial method (magnetic resonance or computed tomography) and the gold standard method (physical method, i.e., dried-femur measurement); horizontal axis shows femoral anteversion values by dried-femur measurement, and vertical axis shows femoral anteversion values by magnetic resonance or computed tomography method. (b and d) (Bland–Altman plot) For comparing the agreement between a trial method (magnetic resonance or computed tomography) and the physical method of femoral anteversion values, the difference of femoral anteversion values from a trial method and the physical method (y-axis) are depicted in relation to the mean of femoral anteversion values from a trial method and the physical method (x-axis).

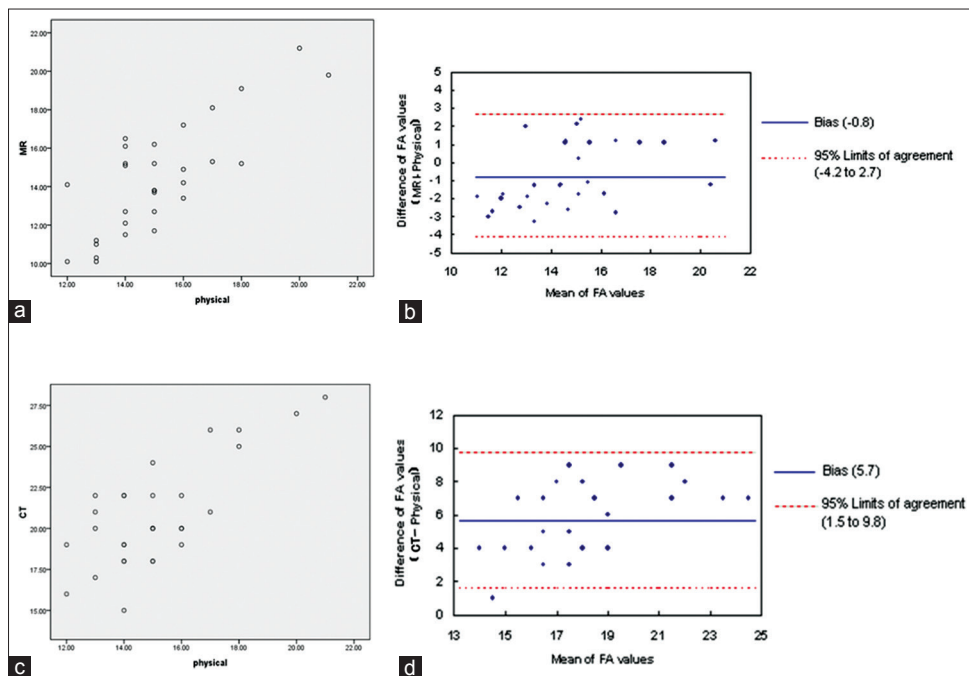


Figure 8: Correlation and Bland–Altman plots for 8-week group using magnetic resonance versus physical measurement (a and b) and computed tomography versus physical measurement (c and d).

system. From Figure 9, we could come to the conclusion that the line-plane angle (FA) is smaller than the plane-plane angle (torsion angle, i.e., the angle measured by CT method). The true FA is not identical to the torsion angle as the femoral neck-shaft angle must be factored in; they would be equal

only if the neck-shaft angle is 90°. The above analysis explains the reason why the mean FA value measured by CT was larger than that measured by MR in our study. This result happens to be consistent to those of studies by Botser *et al.* and Tomczak *et al.*^[12,30] In those studies, large

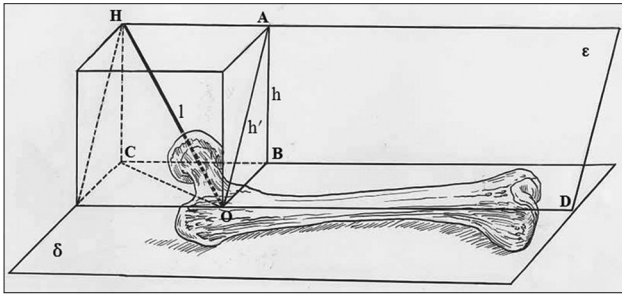


Figure 9: Geometrical structure of femur. Plane δ : A horizontal plane on which the femur was placed, i.e., femoral condylar plane; line OH: Femoral head-neck axis, intersecting plane δ at point O; line OD: the line along femoral shaft axis and within plane δ ; plane ϵ : passing through both line OH and line OD, i.e., anteversion plane; $\angle HOC$ (α): the intersection angle between femoral head-neck axis and condylar plane, a line-plane angle, i.e., the true FA; $\angle AOB$ (β): the included angle between plane δ and plane ϵ , a plane-plane angle, called as torsion angle); $\angle AOH$ (θ) = neck-shaft angle ($\angle HOD$) -90° ; h represents the height of the cuboid; $h' =$ line OA; $l =$ line OH $\therefore \sin\beta = h/h' = l \cdot \sin\alpha / l \cdot \cos\theta$, $\therefore \sin\alpha = \sin\beta \cdot \cos\theta$, $\therefore 0 < \cos\theta < 1$, $\therefore \alpha < \beta$.

correlations between CT and MR anteversion measurements were found, along with higher CT values than those of MR. However, both of them used the 2D imaging modalities, and they cannot explain the reason for the bias value clearly.

At present, 3D-CT FA measurement is used in many hospitals. In our daily clinical work (an overwhelming majority of the patients are children in 3D-CT FA examinations, especially under 2 years of age), we find that CT FA measurement has the following disadvantages. (1) Due to the low-density resolution of CT, the femoral ends in images obtained by the surface-shaded 3D technique contain the ossified parts but no cartilage. Furthermore, children with hip diseases often have delayed development of the ossification nucleus in the femoral head, and the ossification nucleus maybe not in the center of the affected femoral head during development. Hence, only ossified parts cannot represent the true femoral head and femoral condyles in CT method, which will directly affect the accuracy of CT measurement results in small children. On the contrary, MR can show clearly not only the secondary ossification center but also the surrounding cartilage. (2) In current 3D-CT FA measurement, the projection of FA on the axial plane is measured, giving the aforementioned torsion angle. We have demonstrated that the torsion angle is larger than the actual degree of FA in theory. (3) Although in order to reduce radiation exposure, the CT scanning range is divided into two parts, femoral head part and distal femur part, compared with zero-radiation MR, CT examination will inevitably subject child patients to more radiation damage.

The key difference in the childhood and adult skeleton is that children possess epiphyseal cartilage. Thus, in the present study, two different piglet age groups were designed to explore the effects on the trial methods of different ratios of ossification center and epiphyseal cartilage. Our study results showed that in the younger piglet group, with smaller ossification nuclei and more cartilage, the

consistency and correlation between CT and dried-femur measurement results were not as good as those between MR and dried-femur measurement results. In the older piglet group, with bigger ossification nuclei and less cartilage, the consistency and correlation in FA measurement results were similar between CT and MR, compared with the gold standard. This suggests that CT has good reproducibility only when there are more ossification components at both ends of the femur.

3D-FSE-Cube is a promising MR imaging sequence that allows the rapid acquisition of high-spatial resolution isotropic data that can be reformatted in arbitrary planes, making this modality ideal for evaluating body parts with complex regional anatomy.^[31-33] The advantages of the Cube technique include 3D imaging, as well as sensitive and specific imaging of cartilage. In the present study, the application of this MR technique in the 3D volume scanning of piglet femur enabled a full view of the bone and cartilage composition of the femur, from its head to its distal portion, as well as of the adjacent acetabulum. Because of the large scanning range and high resolution of soft tissues, this modality may also be used to detect the surrounding abnormalities and further to explore the correlations between FA abnormalities and pathological changes in bones, cartilages, or ligaments.^[34-39]

The present experimental study investigated piglet FA measurement using different methods. However, as the experimental animals were piglets with shorter femoral necks, measurement errors may have occurred when determining the femoral neck axis in any modality. A longer femoral neck can be seen in pediatric CT/MR examinations; this will facilitate the accurate determination and measurement of the femoral neck axis. Our future study objective is the applications of this experimental study to pediatric patients.

In summary, MR is a unique tool which can achieve noninvasive examination with zero-radiation, multiplane imaging, and high soft tissue resolution. It has great potential clinical value in providing a radiation-free FA measurement method for tens of thousands of pediatric patients. 3D-MR FA measurement can not only accurately measure the degree of FA but also can provide a full view of other abnormalities of the surrounding structures of the femur. If this experimental study method could be used in clinics, we expect it to be a beneficial supplement to the current examination methods in the screening, diagnosis, and treatment of FA-related hip diseases in children.

Financial support and sponsorship

This work was supported by grants from the National Natural Science Foundation of China (Nos. 30871211, 81271538), and Outstanding Scientific Fund of Shengjing Hospital (No. 201208).

Conflicts of interest

There are no conflicts of interest.

REFERENCES

1. Tönnis D, Heinecke A. Diminished femoral antetorsion syndrome: A cause of pain and osteoarthritis. *J Pediatr Orthop* 1991;11:419-31. doi: 10.1097/01241398-199107000-00001.
2. Tönnis D, Heinecke A. Acetabular and femoral anteversion: Relationship with osteoarthritis of the hip. *J Bone Joint Surg Am* 1999;81:1747-70.
3. Gelberman RH, Cohen MS, Shaw BA, Kasser JR, Griffin PP, Wilkinson RH. The association of femoral retroversion with slipped capital femoral epiphysis. *J Bone Joint Surg Am* 1986;68:1000-7.
4. Ito K, Minka MA 2nd, Leunig M, Werlen S, Ganz R. Femoroacetabular impingement and the cam-effect. A MRI-based quantitative anatomical study of the femoral head-neck offset. *J Bone Joint Surg Br* 2001;83:171-6.
5. Jia J, Li L, Zhang L, Zhao Q, Liu X. Three dimensional-CT evaluation of femoral neck anteversion, acetabular anteversion and combined anteversion in unilateral DDH in an early walking age group. *Int Orthop* 2012;36:119-24. doi: 10.1007/s00264-011-1337-0.
6. Murphy SB, Simon SR, Kijewski PK, Wilkinson RH, Griscom NT. Femoral anteversion. *J Bone Joint Surg Am* 1987;69:1169-76.
7. Reikerås O, Bjerkreim I, Kolbenstvedt A. Anteversion of the acetabulum and femoral neck in normals and in patients with osteoarthritis of the hip. *Acta Orthop Scand* 1983;54:18-23. doi: 10.3109/17453678308992864.
8. Ruwe PA, Gage JR, Ozonoff MB, DeLuca PA. Clinical determination of femoral anteversion. A comparison with established techniques. *J Bone Joint Surg Am* 1992;74:820-30.
9. Hernandez RJ, Tachdjian MO, Poznanski AK, Dias LS. CT determination of femoral torsion. *AJR Am J Roentgenol* 1981;137:97-101. doi: 10.2214/ajr.137.1.97.
10. Prasad SS, Bruce C, Crawford S, Higham J, Garg N. Femoral anteversion in infants: A method using ultrasound. *Skeletal Radiol* 2003;32:462-7. doi: 10.1007/s00256-003-0652-y.
11. Wedge JH, Munkacsy I, Loback D. Anteversion of the femur and idiopathic osteoarthritis of the hip. *J Bone Joint Surg Am* 1989;71:1040-3.
12. Tomczak RJ, Guenther KP, Rieber A, Mergo P, Ros PR, Brambs HJ. MR imaging measurement of the femoral antetorsional angle as a new technique: Comparison with CT in children and adults. *AJR Am J Roentgenol* 1997;168:791-4. doi: 10.2214/ajr.168.3.9057536.
13. Guenther KP, Tomczak R, Kessler S, Pfeiffer T, Puhl W. Measurement of femoral anteversion by magnetic resonance imaging – Evaluation of a new technique in children and adolescents. *Eur J Radiol* 1995;21:47-52. doi: 10.1016/0720-048X(95)00684-1.
14. Abel MF, Sutherland DH, Wenger DR, Mubarak SJ. Evaluation of CT scans and 3-D reformatted images for quantitative assessment of the hip. *J Pediatr Orthop* 1994;14:48-53. doi: 10.1097/01241398-199401000-00011.
15. Citak M, Oszward M, O'Loughlin PF, Citak M, Kendoff D, Hüfner T, *et al.* Three-dimensional measurement of femoral antetorsion: Comparison to a conventional radiological method. *Arch Orthop Trauma Surg* 2010;130:513-8. doi: 10.1007/s00402-009-0923-8.
16. Davids JR, Marshall AD, Blocker ER, Frick SL, Blackhurst DW, Skewes E. Femoral anteversion in children with cerebral palsy. Assessment with two and three-dimensional computed tomography scans. *J Bone Joint Surg Am* 2003;85-A:481-8.
17. Kim JS, Park TS, Park SB, Kim JS, Kim IY, Kim SI. Measurement of femoral neck anteversion in 3D. Part 1: 3D imaging method. *Med Biol Eng Comput* 2000;38:603-9. doi: 10.1007/BF02344864.
18. Kim JS, Park TS, Park SB, Kim JS, Kim IY, Kim SI. Measurement of femoral neck anteversion in 3D. Part 2: 3D modelling method. *Med Biol Eng Comput* 2000;38:610-6. doi: 10.1007/BF02344865.
19. Liu D, Ma R, Ji S. Measurement of femoral neck anteversion with three-dimensional reconstruction by spiral-CT. *Chin J Pediatr Surg* 2002;23:526-30. doi: 10.3760/cma.j.issn.0253-3006.2002.06.016.
20. Brody AS, Frush DP, Huda W, Brent RL; American Academy of Pediatrics Section on Radiology. Radiation risk to children from computed tomography. *Pediatrics* 2007;120:677-82. doi: 10.1542/peds.2007-1910.
21. Donnelly LF. Reducing radiation dose associated with pediatric CT by decreasing unnecessary examinations. *AJR Am J Roentgenol* 2005;184:655-7. doi: 10.2214/ajr.184.2.01840655.
22. Shah NB, Platt SL. ALARA: Is there a cause for alarm? Reducing radiation risks from computed tomography scanning in children. *Curr Opin Pediatr* 2008;20:243-7. doi: 10.1097/MOP.0b013e3282ffaf2.
23. Larson DB, Johnson LW, Schnell BM, Goske MJ, Salisbury SR, Forman HP. Rising use of CT in child visits to the emergency department in the United States, 1995-2008. *Radiology* 2011;259:793-801. doi: 10.1148/radiol.11101939.
24. Mazrani W, McHugh K, Marsden PJ. The radiation burden of radiological investigations. *Arch Dis Child* 2007;92:1127-31. doi: 10.1136/adc.2006.101782.
25. Frush DP, Donnelly LF, Rosen NS. Computed tomography and radiation risks: What pediatric health care providers should know. *Pediatrics* 2003;112:951-7. doi: 10.1542/peds.112.4.951.
26. Dunn PM, Gardiner HM. Screening for congenital dislocation of the hip. *Lancet* 1991;337:1096-7. doi: 10.1016/S0140-6736(05)72106-1.
27. Schenkman L. Radiology. Second thoughts about CT imaging. *Science* 2011;331:1002-4. doi: 10.1126/science.331.6020.1002.
28. Koenig JK, Pring ME, Dwek JR. MR evaluation of femoral neck version and tibial torsion. *Pediatr Radiol* 2012;42:113-5. doi: 10.1007/s00247-011-2206-0.
29. Mootha AK, Saini R, Dhillon MS, Aggarwal S, Kumar V, Tripathy SK. MRI evaluation of femoral and acetabular anteversion in developmental dysplasia of the hip. A study in an early walking age group. *Acta Orthop Belg* 2010;76:174-80.
30. Botser IB, Ozoude GC, Martin DE, Siddiqi AJ, Kuppuswami S, Domb BG. Femoral anteversion in the hip: Comparison of measurement by computed tomography, magnetic resonance imaging, and physical examination. *Arthroscopy* 2012;28:619-27. doi: 10.1016/j.arthro.2011.10.021.
31. Stevens KJ, Busse RF, Han E, Brau AC, Beatty PJ, Beaulieu CF, *et al.* Ankle: Isotropic MR imaging with 3D-FSE-cube – Initial experience in healthy volunteers. *Radiology* 2008;249:1026-33. doi: 10.1148/radiol.2493080227.
32. Stevens KJ, Wallace CG, Chen W, Rosenberg JK, Gold GE. Imaging of the wrist at 1.5 Tesla using isotropic three-dimensional fast spin echo cube. *J Magn Reson Imaging* 2011;33:908-15. doi: 10.1002/jmri.22494.
33. Kijowski R, Davis KW, Woods MA, Lindstrom MJ, De Smet AA, Gold GE, *et al.* Knee joint: Comprehensive assessment with 3D isotropic resolution fast spin-echo MR imaging – Diagnostic performance compared with that of conventional MR imaging at 3.0 T. *Radiology* 2009;252:486-95. doi: 10.1148/radiol.2523090028.
34. Wakabayashi K, Wada I, Horiuchi O, Mizutani J, Tsuchiya D, Otsuka T. MRI findings in residual hip dysplasia. *J Pediatr Orthop* 2011;31:381-7. doi: 10.1097/BPO.0b013e31821a556e.
35. Sher I, Umans H, Downie SA, Tobin K, Arora R, Olson TR. Proximal iliotibial band syndrome: What is it and where is it? *Skeletal Radiol* 2011;40:1553-6. doi: 10.1007/s00256-011-1168-5.
36. Sanders JO, Otsuka NY, Martus JE. What's new in pediatric orthopaedics. *J Bone Joint Surg Am* 2015;97:344-50.
37. Kijowski R, Gold GE. Routine 3D magnetic resonance imaging of joints. *J Magn Reson Imaging* 2011;33:758-71. doi: 10.1002/jmri.22342.
38. Steinert L, Zanetti M, Hodler J, Pfirrmann CW, Dora C, Saupé N. Are radiographic trochanteric surface irregularities associated with abductor tendon abnormalities? *Radiology* 2010;257:754-63. doi: 10.1148/radiol.10092183.
39. Chhabra A, Nordeck S, Wadhwa V, Madhavapeddi S, Robertson WJ. Femoroacetabular impingement with chronic acetabular rim fracture – 3D computed tomography, 3D magnetic resonance imaging and arthroscopic correlation. *World J Orthop* 2015;6:498-504. doi: 10.5312/wjo.v6.i6.498.